Nuclear Structure of ^{104,106,108}Sn Isotopes Using the NuShell Computer Code

Khalid S. Jassim

Department of Physics, College of Education for Pure Science,
University of Babylon, PO Box 4, Hillah-Babylon, Iraq
(Received February 21, 2012; Revised August 13, 2012)

Shell model calculations for ^{104,106,108}Sn are preformed using the *NuShell code* for windows with an effective interaction based on the CD-Bonn nucleon-nucleon interaction. The level schemes are compared with the available experimental data up to 3.98, 11.319, and 4.256 MeV in ^{104}Sn, ^{106}Sn, and ^{108}Sn, respectively. Very good agreement was obtained for each of the nuclei, especially for ^{106}Sn. The electron scattering form factor, transition probabilities B (E2; $0^+ \rightarrow 2_1^+$), and charge density distribution have been found using a shell model calculation.

I. INTRODUCTION

The region of light Sn isotopes between the $N = 50$ and 82 shell closures provide the longest chain of semi-magic nuclei accessible to nuclear structure studies. Both in the neutron valence space of a full major shell and with emphasis on excitations of the $Z = 50$ core Sn isotopes, it has been intensively investigated from both experimental and theoretical perspectives. The main goal has been to study the excitation mechanisms around the exotic isotope ^{100}Sn, the heaviest symmetric double magic nucleus recently produced in nuclear fragmentation reactions [1, 2]. The perturbative many-body method used to calculate such an effective interaction, appropriate for nuclear structure calculations at low and intermediate energies, starts with the free nucleon-nucleon interaction. CD-Bonn and Nijmegen1 two-body effective nucleon-nucleon interactions are used to calculate the effective NN interactions in the desired model space. The effect of the repulsive core of the NN potential at close range, which is unsuitable for a perturbative treatment, is taken into account in the effective interaction. One can then derive expressions for the effective interactions and transition operators via the many-body G-matrix method [3].

The simplest approach in analysing the spectra of light Sn isotopes is to consider ^{100}Sn as an inert core and to treat only the neutron degrees of freedom, using the single-particle orbits of the $N = 50$–82 shell as a model space, i.e., the orbits $1g_{7/2}$, $2d_{5/2}$, $2d_{3/2}$, $3s_{1/2}$, and $1h_{11/2}$. Extensive shell model calculations have been performed along this line [4]; using the Lanczos iteration method states for as many as 12 extra-core neutrons have been calculated. Similar studies have also been done in heavy Sn isotopes [5] and in the $N = 82$ isotones [6], where systems with up to 14 valence particles have been studied. The structure of neutron-rich nuclei with a few nucleons beyond ^{132}Sn [7] have been investigated by means of large-scale shell-model calculations. The results show evidence of hexadecupole correlation in addition to octupole correlation in this mass region.

On the one hand, the results still deviate significantly from theoretical predictions and, on the other hand, the results indicate a decreasing trend of the energy levels with increasing number of valence particles outside of the ^{100}Sn core. Experimentally, the nuclear properties of ^{100}Sn are only indirectly known [7, 8], although its existence has already been confirmed [9–11]. Properties of the 2^+ states around ^{132}Sn have been also studied by Terasaki *et al.* [6] in a separable quadrupole-plus-pairing model.

A large-scale shell model calculation was carried out in the Sn100pn model space with the Sn100pn interaction. This interaction was obtained from a realistic interaction developed by Brown *et al.* [6] starting with a G matrix derived from the CD-Bonn nucleon-nucleon interaction. There are three parts in this interaction, which are the proton-proton (Sn100pp), neutron-neutron (Sn100nn), and proton-neutron (Sn100pn) interactions, along with the coulomb interaction (Sn100co) between the protons. In this work, I am interested in the Sn isotopes only, the neutron-neutron part, i.e., only Sn100nn was relevant for my calculation. The calculations have been performed using doubly magic 100Sn as the core and the valance neutrons (4, 6, and 8) distributed over the single particle-orbits $1s_{1/2}$, $2d_{5/2}$, $2d_{3/2}$, $2g_{7/2}$, and $1h_{11/2}$. The neutron single-particle energies are -8.7167 MeV, -10.6089 MeV, -8.6944 MeV, -10.2893 MeV, and -8.8152 MeV for the $3s_{1/2}$, $2d_{5/2}$, $2d_{3/2}$, $1g_{7/2}$, and $1h_{11/2}$ orbitals, respectively [6]. The energy level results and transition probabilities are compared with the experimental levels, as shown in Figures 1, 2, and 3.

II. RESULTS AND DISCUSSION

II-1. Energy Levels and transition probabilities

In order to estimate the energy levels in $^{104-106-108}$Sn, we have performed shell model calculations using the *NuShell computer code* for windows [12]. We are interested in positive and some negative parity states of ^{106}Sn with isoscalar T_z=4, for the valance neutron states ($1g_{7/2}$, $2d_{5/2}$, $2d_{3/2}$, $3s_{1/2}$, and $1h_{11/2}$) outside the core ^{100}Sn.

The energy levels spectra of ^{104}Sn are presented in Figure 1. Our results are reported and plotted in the first column and compared with the experimental spectrum in the second column. It can seen that the agreement is excellent for the states 0^+ and 10^+, and there is good agreement for the states 2^+, 4^+, and 8^+ in comparison with the experimental results taken from Ref. [13].

The calculated energy levels in the ^{106}Sn CD-Bonn effective interaction are compared with the experimental data, as shown in Figure 2. The agreement is excellent for the $J^\pi = 0_1^+$, 4_1^+, 6_1^+, 8_1^+, 10_2^+, 11_1^+, and 22_1^+ states in comparison with the data from Ref. [14]. Three energy levels with negative parity states have been calculated for ^{106}Sn, as shown in Figure 2. These theoretical values are 4.456 MeV for the 11_1^- state, 5.426 MeV for the 14_1^- state, and 6.108 MeV for the 15_1^- state, and the absolute differences from the experimental data [14] are 1.087, 2.172, and 1.277 MeV, respectively. The calculation of the energy levels for negative parity starts to deviate from the experimental values, and this reflects the inadequacy of the model space. More negative parity results for the Sn isotopes will be published in a forthcoming paper; also researchers are invited to calculate these levels

using another effective interaction, such as the delta interaction or modified surface delta interaction.

Figure 3 shows theoretical and experimental values for the energy levels of ^{108}Sn, the present results on the energy levels agree well with the experimental data [15] at 0^+, 2_1^+, 6_1^+, 4_3^+, 3_1^+, and 8_2^+.

The transition probabilities B (E2; $0^+ \rightarrow 2_1^+$) results are compared with the experimental data in Table I. It can be seen that the theoretical B (E2) values reproduce the data quite well.
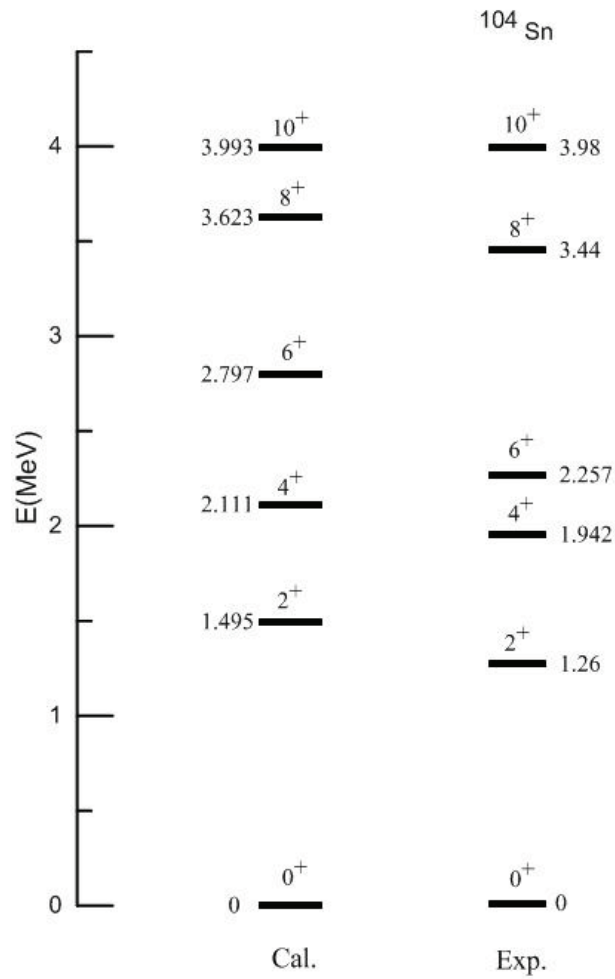
FIG. 1: Energy levels of ^{104}Sn. Experimental data from Ref. [14] are compared to the shell model results with the CD-Bonn effective interaction.
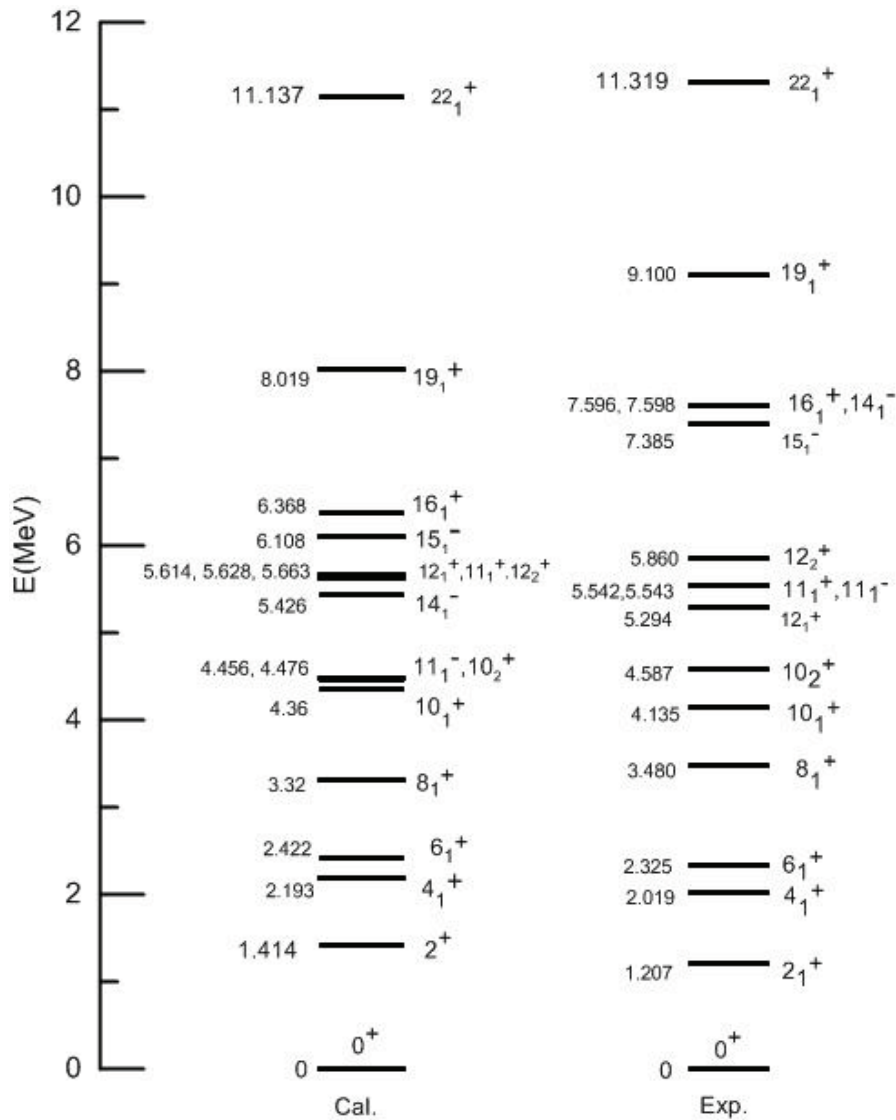
FIG. 2: Energy levels of ^{106}Sn. Experimental data from Ref. [15] are compared to the shell model results with the CD-Bonn effective interaction.

II-2. Electron Scattering Form Factors

The longitudinal and transverse electron scattering form factors for ^{104}Sn and ^{106}Sn are calculated with the residual interaction being based on the CD-Bonn renormalized G matrix elements for different states: 2_1^+ (1.105 MeV) for ^{104}Sn and 10_1^+ (1.04 MeV), and 4_1^+ (2.193 MeV) for ^{106}Sn.

Figures (4) and (5) show the C2 and E2 form factors, respectively, for the transition from 0_1^+ to 2_1^+ with excitation energy 1.495 MeV. From Figure 4, we note that three maxi-
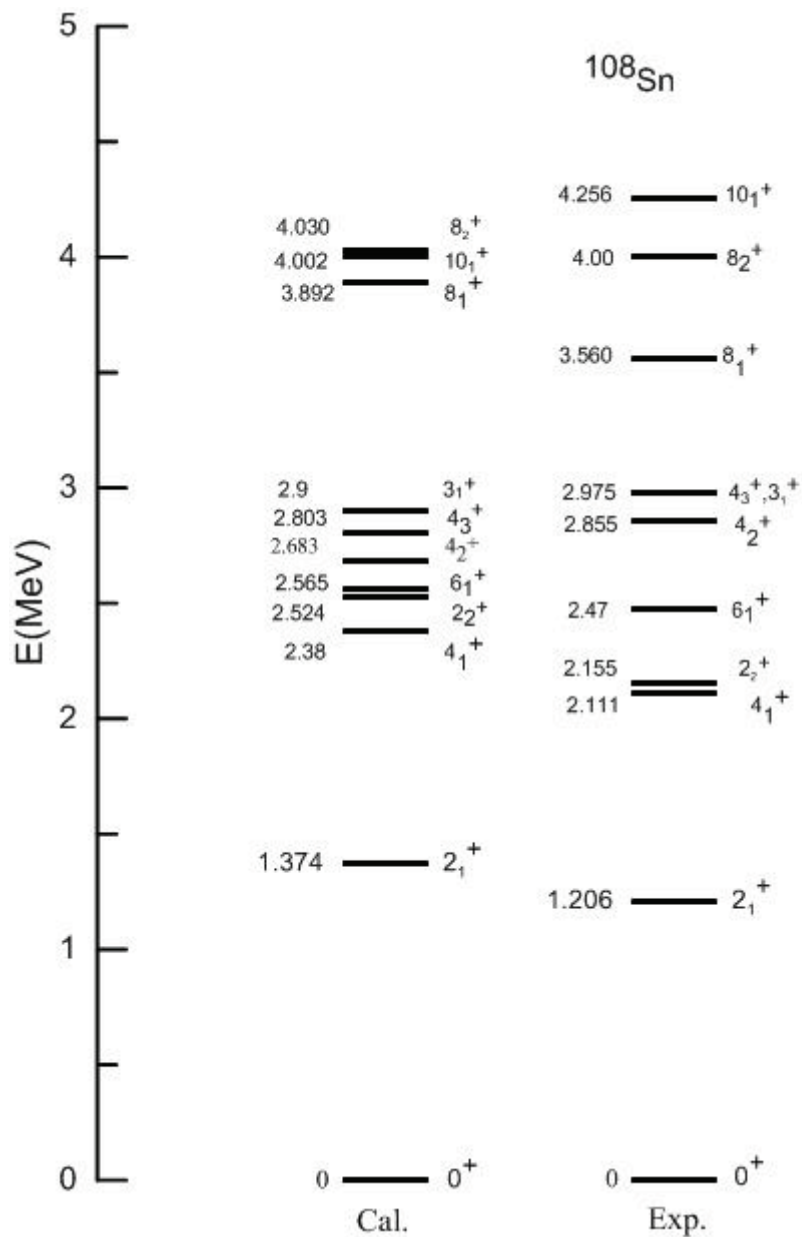
FIG. 3: Energy levels of ^{108}Sn. Experimental data from Ref. [16] are compared to the shell model results with the CD-Bonn effective interaction.

mum diffractions for electrons scattered by the charge distribution and current inside the nucleus at the momentum transfers $q = 0.5$ fm^{-1}, 1.2 fm^{-1}, and 1.7 fm^{-1}. From Figure 5, we note two maximum diffractions at the momentum transfers $q = 0.6$ fm^{-1} and 1.6 fm^{-1}.

The C2 form factors for the transition from 8_1^+ to 10_1^+ at 1.04 MeV for ^{106}sn are shown
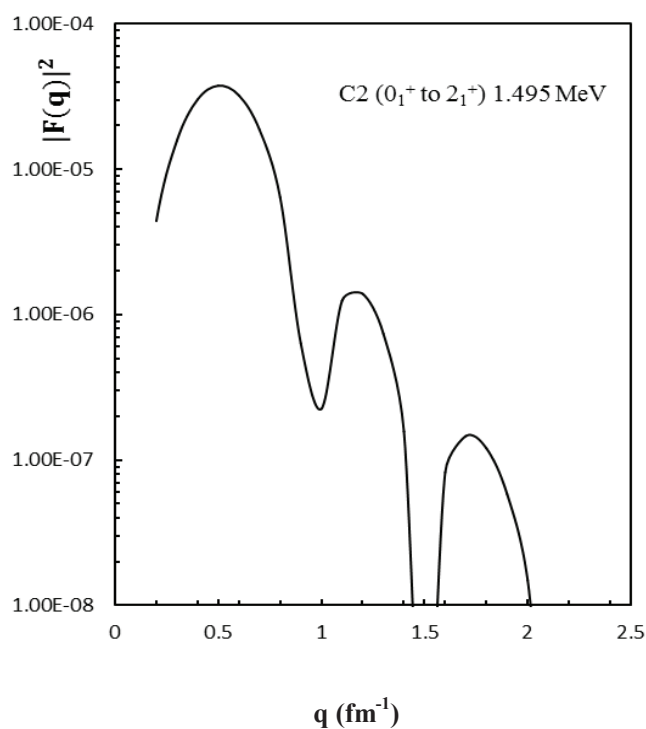
FIG. 4: The Coulomb (C2) form factors for the transition to the 2_1^+ (1.495 MeV) state in ^{104}Sn.
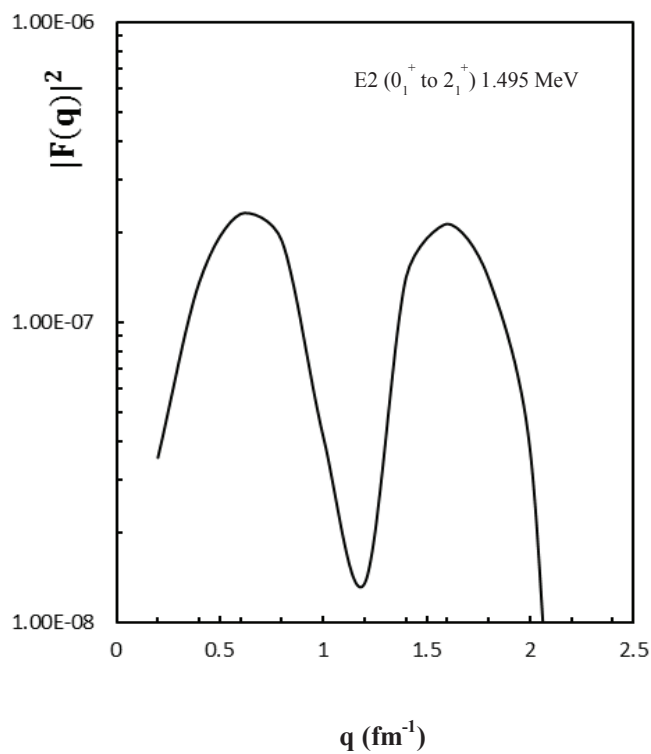

FIG. 5: The transverse (E2) form factors for the transition to the 2_1^+ (1.495 MeV) states in ^{104}Sn.
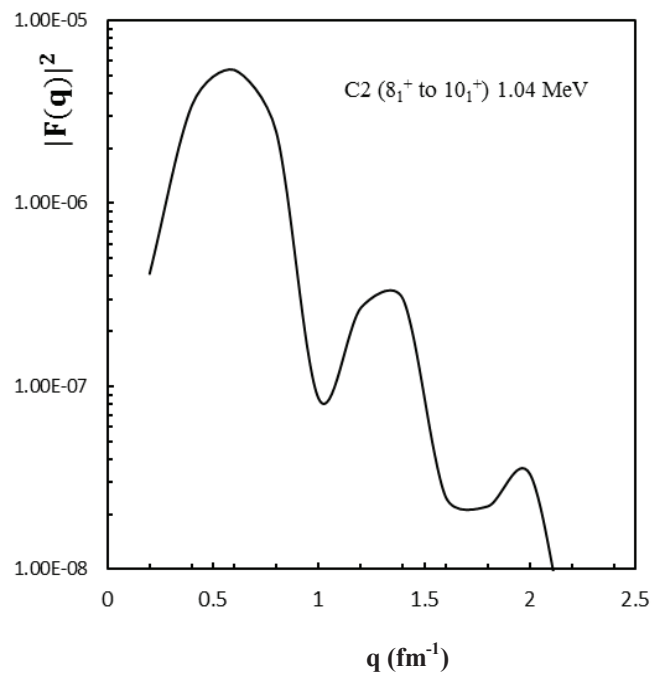
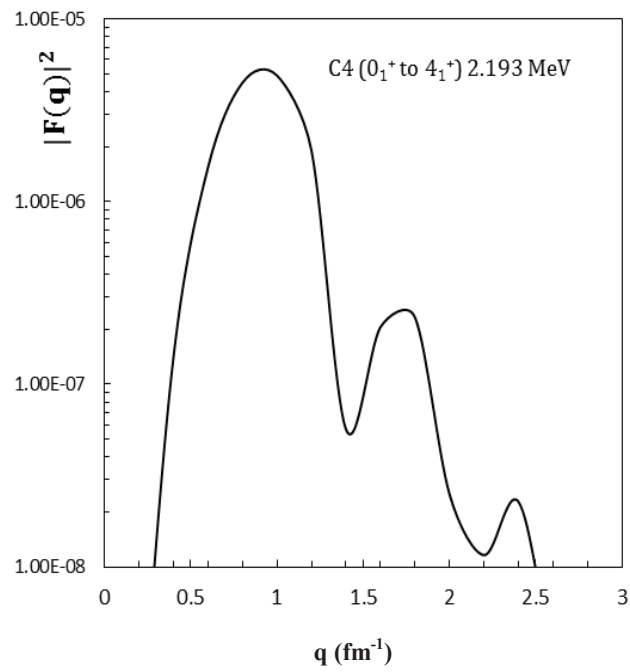FIG. 6: The Coulomb (C2) form factors for the transition to the 10_1^+ (1.04 MeV) states in ^{106}Sn.

FIG. 7: The longitudinal (C4) form factors for the 4_1^+ (2.193 MeV) state in ^{106}Sn.
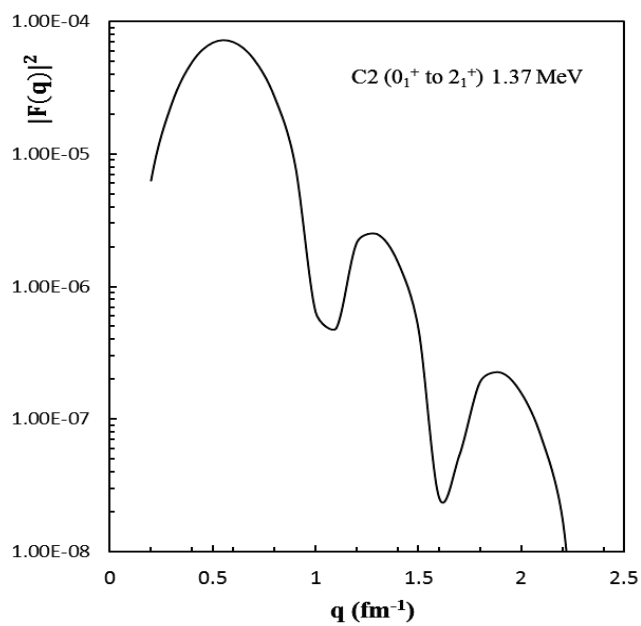
FIG. 8: The longitudinal (C2) form factors for the 2^+_1 (1.37 MeV) state in ^{108} Sn.
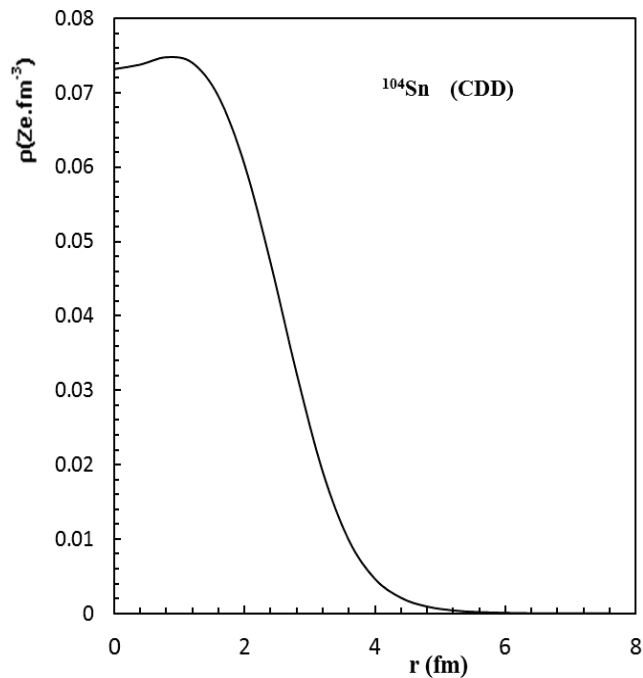

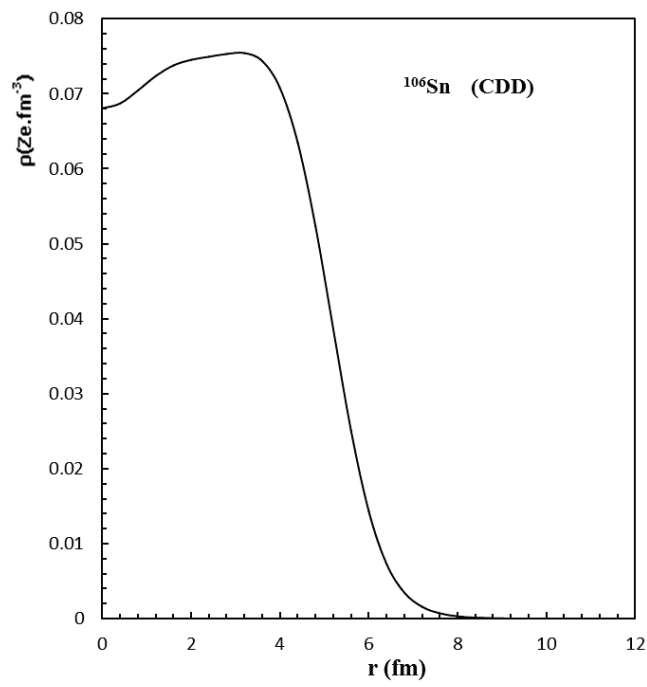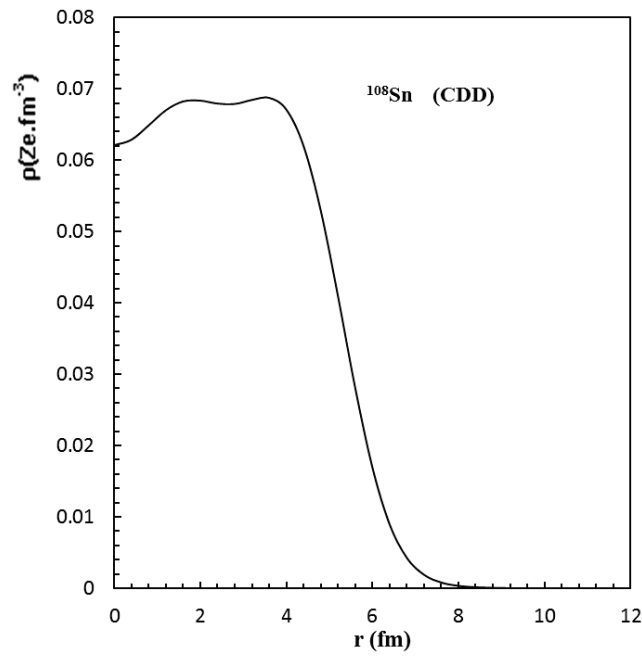FIG. 9: Dependence of the CDD on the r (fm) for ^{104}Sn.

FIG. 10: Dependence of the CDD on r (fm) for ^{106}Sn.

FIG. 11: Dependence of the CDD on r (fm) for ^{108}Sn.

TABLE I: Comparison of the B (E2; $0^+ \rightarrow 2_1^+$) values, obtained from the shell model calculations with the experimental values in e^{2}b^2 for even Sn isotopes. The experimental data have been taken from Ref. [17, 18]

Isotope	Exp.	Present work
^{104}Sn	—	0.0849
^{106}Sn	0.240	0.3504
^{108}Sn	0.230	0.1979

in Figure 6. The maximum diffraction for the scattered electrons are at the momentum transfer values $q = 0.6$ fm^{-1}, 1.4 fm^{-1}, and 2 fm^{-1}. The minimum diffraction values are at $q = 1$ fm^{-1} and 1.8 fm^{-1}. As mentioned previously, the experimental data are unavailable at the literature in the mean time; therefore, these results cannot be comparable with the experimental results.

Figure 7 represents the relation between the C4 form factors as a function of momentum transfer for the state from 0_1^+ to 4_1^+ at excitation energy 2.193 MeV. The diffraction maxima for the scattered electrons are at the momentum transfer values $q = 1$ fm^{-1}, 1.8 fm^{-1}, and 2.4 fm^{-1}. The maximum diffraction values are at $q = 1$ fm^{-1} and 2.2 fm^{-1}. The minimum diffraction values at $q = 1.4$ fm^{-1} and 2.2 fm^{-1}.

The longitudinal (C2) form factor for the 2_1^+ (1.37 MeV) state of ^{108}Sn is shown in Figure 8. The maximum diffraction values are at $q = 0.6$ fm^{-1}, 1.3 fm^{-1}, and 1.9 fm^{-1}. The minimum diffraction for scattered electrons are at the momentum transfer values $q = 1.1$ fm^{-1} and 1.6 fm^{-1}.

II-3. Charge density distribution (CDD)

The dependence of the CDD ρ (Ze.fm^{-3}) on r (fm) for ^{104}Sn, ^{106}Sn, and ^{108}Sn nuclei are displayed in Figures 9, 10, and 11, respectively. We note that the CDD at the centre of the nucleus ($r = 0$ fm) for ^{104}Sn, ^{106}Sn, and ^{108}Sn are 7.32×10^{-2} (Ze.fm^{-3}), 6.81×10^{-2} (Ze.fm^{-3}), and 6.21×10^{-2} (Ze.fm^{-3}), respectively; they began to increase up to 7.48×10^{-2} (Ze.fm^{-3}) at $r = 0.8$ fm, 7.54×10^{-2} (Ze.fm^{-3}) at $r = 3.2$ fm, and 6.87×10^{-2} (Ze.fm^{-3}) at $r = 3.6$ fm, respectively. After that the CDD began decreasing down to zero at $r = 4.8$ fm, 8 fm, and 8.4 fm, respectively.

III. SUMMARY

The nuclear structure (energy level, transition probabilities, form factors, and CDD) calculations with an effective interaction based on the CD-Bonn nucleon-nucleon interaction were performed for ^{104,106,108}Sn using the *NuShell code* for windows. The energy levels results are compared with the experimental levels. The agreement between the calculated and experimental excitation energies up to 3.98, 11.319, and 4.256 MeV in ^{104}Sn, ^{106}Sn,

and ^{108}Sn, respectively, are very good. The electron scattering form factor r and the charge density distribution are found using the shell model calculation. These results are not compared with the experimental results, because the experimental data are unavailable in the literature at the present time.

References

[1] M. Lewitowicz *et al.*, Phys. Lett. **B332**, 20 (1994).
[2] R. Schneider *et al.*, Zeit. Phys. **A348**, 241 (1994).
[3] M. Hjorth-Jensen *et al.*, Phys. Rep. **261**, 125 (1995).
[4] T. Engeland, M. Hjorth-Jensen, A. Holt, and E. Osnes, Phys. Scripta **T56**, 58 (1995).
[5] T. Engeland, M. Hjorth-Jensen, A. Holt, and E. Osnes, in *Proceedings of the International Workshop on Double-beta Decay and Related Topics*, eds. H. V. Kapdor and S. Stoica (World Scientific, Singapore, 1996), p. 421.
[6] B. A. Brown *et al.*, Phys. Rev. C **71**, 044317 (2005).
[7] H. Jin *et al.*, Phys. Rev. C **84**, 044324 (2011).
[8] M. Lipoglavsek *et al.*, Phys. Lett. **B440**, 246 (1998).
[9] M. G'orska *et al.*, Phys. Rev. C **58**, 108 (1998).
[10] A. Blazhev *et al.*, Phys. Rev. C **69**, 64304 (2004).
[11] M. Lewitowicz *et al.*, Phys. Lett. **B332**, 20 (1994).
[12] R. Schneider *et al.*, Z. Phys. **A348**, 241 (1994).
[13] B. A. Brown and W. D. M. Rae, MSU-NSCL report (2007).
[14] J. Blachot, Nuclear Data Sheets **108**, 2035 (2007). doi: 10.1016/j.nds.2007.09.001
[15] D. D. Frenne and A. Negret, Nucl. Data Sheets **109**, 943 (2008). doi: 10.1016/j.nds.2008.03.002
[16] J. Blachot, Nucl. Data Sheets **91**, 135 (2000). doi: 10.1006/ndsh.2000.0017
[17] A. Banu *et al.*, Phys. Rev. C **72**, 061305(6) (2005).
[18] C. Vaman *et al.*, Phys. Rev. Lett. **99**, 162501 (2007).